Dentomaxillofacial Radiology (1998) 27, 140–150
© 1998 Stockton Press All rights reserved 0250–832X/98 $12.00
http://www.stockton-press.co.uk/dmfr

Observer-independent registration of perspective projection prior to subtraction of *in vivo* radiographs

TM Lehmann[1], K Gröndahl[2], H-G Gröndahl[2], W Schmitt[3] and K Spitzer[1]

[1]*Institute of Medical Informatics, Aachen University of Technology (RWTH), Aachen, Germany;* [2]*Department of Oral Diagnostic Radiology, Göteborg University, Göteborg, Sweden;* [3]*Department of Oral Surgery, University of Bonn, Bonn, Germany*

Objectives: To prove that the model of perspective projection allows precise registration of intra-oral radiographs regardless of whether they have been acquired with or without individual adjustment aids and independent of the human observer or computer algorithm marking corresponding landmarks in the images and, based on *in vivo* radiographs, to introduce and evaluate a model-based registration method.
Methods: Five observers (three experts and two non-experts) were asked to define corresponding points in 24 pairs of *in vivo* dental radiographs from the same region of the same patient. The landmarks were used to fit the model of perspective projection applying the least squares method. Misplaced landmarks were detected and suppressed by analysing the quality of all subsets of landmarks with respect to the minimal residual (leaving one out method). In addition, local correlation was used to optimize the quality of registration as well as observer independence.
Results: Using six or more corresponding landmarks in both radiographs the correlation of the images registered was >0.95 (S.D. <0.063) irrespective of the observers' expertise.
Conclusions: Perspective projection is a reliable model for sequentially acquired intra-oral radiographs. The co-ordinates of anatomical landmarks are useful for determining the parameters of perspective projection. Local correlation and leaving one out techniques improve the geometrical adjustment as well as observer independence. Registration is nearly independent of the actual position of the landmarks and hence independent of the observer. Our algorithm will also be useful for registration techniques based on automatically detected landmarks.

Keywords: image processing, computer assisted; radiography, dental

Introduction

In radiographic diagnosis, images of the same region acquired with similar or different modalities over short or long periods of time often have to be compared. Considering only one modality, problems arise if images differ in contrast and/or projection, regardless of whether the comparison is done by experts or with automatic computer algorithms.[1]

For example, spatial registration is a major problem in dental radiology when digital radiographs from the same region have to be compared to assess changes occurring over a time interval. Digital subtraction techniques are the best noninvasive tools for diagnosing small changes but they require perfect geometrical match.[2–5] Since individual mechanical devices such as bite blocks are cumbersome to use clinically and have been shown to be reliable for only periods of less than one year,[6] algorithms for automatic registrations of dental radiographs have been presented.[7–9] These algorithms are restricted to the detection of movements such as rotations, scalings and/or translations (RST-movements). However, RST-movements are insufficient to describe intra-oral radiology if individual adjustment aids are sacrificed. Therefore, these techniques still do not enable automatic alignment prior to subtraction of clinical radiographs.

Manual registration techniques are usually based on landmarks which are marked in both images to be registered. Using deformation algorithms, the corresponding points are mapped exactly onto each other

Correspondence to: Dipl.-Ing. Thomas M. Lehmann, Institut für Medizinische Informatik und Biometrie, Aachen University of Technology (RWTH), 52057 Aachen, Germany
Received 4 August 1997; accepted 26 November 1997

while the others are interpolated based on the triangulation of the spatial domain[10] or on energy minimization models. The latter algorithms are also known as thin-plate spline warping.[11] This group of warping techniques has two major drawbacks when applied to medical images. On one hand, the transform of every triangle in the image depends on the neighbouring fixed-points which usually differ. This complicates quantitative measurements after registration and may cause artefacts in the transition of two triangles.[10] On the other hand, the result of the registration is extremely dependent on the actual positioning of corresponding points and therefore, image warping is highly observer-dependent.

In dental radiology, reference point-based algorithms have been used previously to achieve sufficient overlap of intra-oral radiographs prior to their subtraction.[12] However, the influence of the number of landmarks or their positions, depending on the human observer who is placing them, has not been analysed.

Our hypothesis is that the model of perspective projection allows precise registration of intra-oral radiographs regardless of whether they have been acquired with or without individual adjustment aids and that it is independent of the human observer or computer algorithm marking corresponding landmarks in the images. In common with other techniques, our approach is also based on corresponding landmarks, but in contrast, the co-ordinates are used to fit a certain model of geometrical projection.

The part material and methods of this paper is organized as follows. The kind and complexity of the model of geometrical projection is derived in Paragraph 2.1. Our idea using the term *landmark* is defined in Paragraph 2.2. The determination of the model's parameters based on those landmarks is explained in Paragraph 2.3 while the mathematics and implementation details of our algorithm are derived in the appendix. Paragraphs 2.4 and 2.5 describe optimization techniques which are applied to improve the observer-independence. The radiographic material and how it is used to evaluate our method is described in Paragraph 2.6.

Materials and Methods

Theoretical background perspective projection

In intra-oral radiography the focus spot is usually smaller than 1 mm^2, allowing the approximation that the X-ray beam emanates from a point source. Presupposing fixed positions of the X-ray tube and the patient but a sensor that may be rotated and translated in all directions in three dimensional space, each pixel (x,y) in the image, acquired before the sensor's displacement, is transformed into the position (x',y') in the image obtained afterwards (Figure 1). This reversible geometric transform is known as perspective projection and is given by:[13]

$$x' = \frac{a_1 x + a_2 y + a_3}{a_7 x + a_8 y + 1} \text{ and } y' = \frac{a_4 x + a_5 y + a_6}{a_7 x + a_8 y + 1} \qquad (1)$$

where the parameters $a_1 \ldots a_8$ determine the projection. Less complex models could be derived from perspective projection. If $a_7 = a_8 \equiv 0$, equation (1) yields affine transforms. Rotations are modeled by the parameters a_1, a_2 and a_4, a_5 while a_3, a_6 describe translations in x and y-direction, respectively.

In practice, all the components of the system such as tube, object, and sensor may be moved and/or rotated between the acquisition of two *in vivo* radiographs. The direction of the X-ray beam in relation to the patient will change and, due to the summation effects of X-ray imaging, a different image will be obtained. In these cases, the projection is not reversible.

Total, three rotations (R) and three translations (T) of all three components are possible. They result in 18 displacement vectors (Table 1). Some of the vectors are negligible, e.g. rotations of the tube (X) around the projection axis (XR_z). Others are linear-dependent. For example, geometric distortions caused by the movement of the patient (O) perpendicular to the central beam ($+OT_x$) are identical to those obtained by moving both tube and sensor (S) in the opposite direction ($-ST_x - XT_x$). Therefore, the set of 18 vectors can be reduced to eight linear-independent basic vectors, the six possible movements of the sensor and the two patient shifts across the projection axis.

Table 1 lists all displacement vectors and their approximations. Note that in oral radiology the smallest focus-patient distance is given by the length of the spacer-cone and is usually larger than 20 cm while the patient-sensor distance is shorter than 1 cm (Figure 1). Therefore, small patient movements perpendicular to the central beam ($OT_{x,y}$) can be approximated by sensor movements in the same direction ($ST_{x,y}$). Following this approximation, the remaining six basic vectors exclusively address displacements of the sensor which are exactly described by the model of perspective projection. In other words, the perspective projection defined in equation (1) approximates intra-oral radiography.

Landmarks

An *image landmark*, also referred to as a corresponding or reference point, is defined by a dominant pixel in a grey scale image which is highlighted by strong local

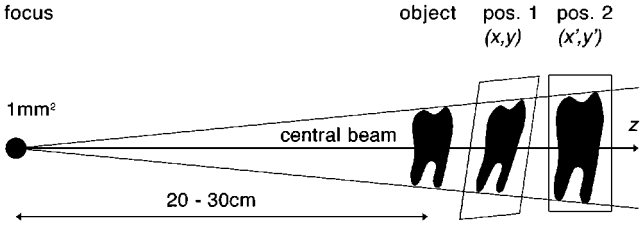

Figure 1 X-rays emanate from the tube, pass through the object and then expose the image receptor. Positions 1 and 2 describe the location of the receptor acquiring the reference and the subsequent radiographs respectively

contrasts. Figure 2 exemplifies (image) landmarks in dental radiographs. The top row of Figure 2 contains the original radiographs while small white crosses are overlaid in the bottom row to indicate the landmarks' positions. Sharp corners between edges in teeth, fillings and implants as well as in the trabecular pattern enable recognizable landmarks to be determined.

This definition of landmarks in two-dimensional pictures differs from *anatomical landmarks* which are usually defined in a three-dimensional environment. Of course, X-ray imaging projects anatomical landmarks into image landmarks. However, not every anatomical landmark results in an image landmark and most image landmarks have no corresponding anatomical landmark. For example, the edge of a tooth in an image corresponds to the side view of a plane. The same goes for implants where an image landmark corresponds to a point on a cylinder.

Nevertheless, the coordinates (x,y) and (x',y') of corresponding image landmarks can be used to determine the parameters a_i of the perspective projection by mapping one radiograph onto its reference. Using four pairs of landmarks, inversion of equation (1) yields the following system of equations:

Table 1 Translations (T) and rotations (R) of the sensor (S), object (O), and X-ray tube (X) results in reversible and irreversible projections

Displacement	*Projection*	*Linear combination*	*Approximation*
ST_x	reversible	basic-vector	–
ST_y	reversible	basic-vector	–
ST_z	reversible	basic-vector	–
SR_x	reversible	basic-vector	–
SR_y	reversible	basic-vector	–
SR_z	reversible	basic-vector	–
OT_x	irreversible	basic-vector	$-ST_x$
OT_y	irreversible	basic-vector	$-ST_y$
OT_z	irreversible	$-ST_z-XT_z$	$-ST_z$
OR_x	irreversible	$-XT_y-XT_z-XR_x+ST_y+ST_z-SR_x$	$+ST_y+ST_z-SR_x$
OR_y	irreversible	$+XT_x-XT_z-XR_y-ST_x+ST_z-SRy$	$-ST_x+ST_z-SR_y$
OR_z	reversible	$-SR_z-XR_z$	$-SR_z$
XT_x	irreversible	$-ST_x-OT_x$	$-ST_x$
XT_y	irreversible	$-ST_y-OT_y$	$-ST_y$
XT_z	negligible	–	0
XR_x	negligible	–	0
XR_y	negligible	–	0
XR_z	negligible	–	0

Some movements have only a little influence on the projection. They are labeled negligible[14]

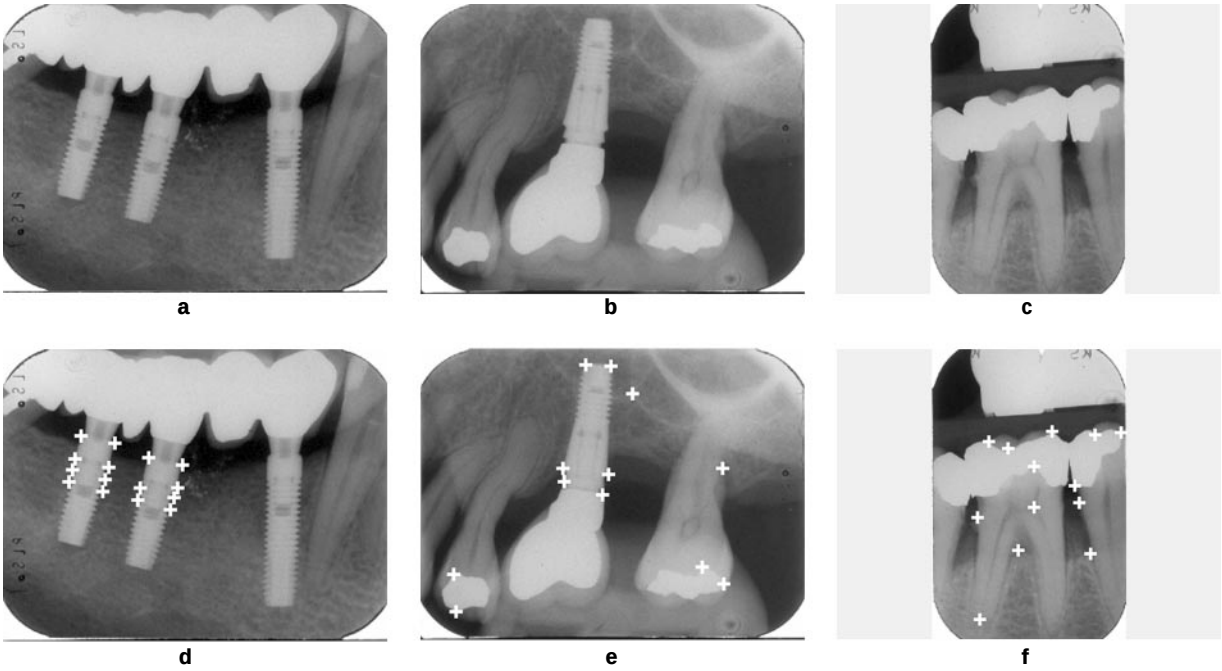

Figure 2 Landmarks in the radiographs (a), (b) and (c) have been marked by an observer with small white crosses as shown in (d), (e) and (f)

$$\begin{pmatrix} x_1 & y_1 & 1 & 0 & 0 & 0 & -x'_1x_1 & -x'_1y_1 \\ 0 & 0 & 0 & x_1 & y_1 & 1 & -y'_1x_1 & -y'_1y_1 \\ x_2 & y_2 & 1 & 0 & 0 & 0 & -x'_2x_2 & -x'_2y_2 \\ 0 & 0 & 0 & x_2 & y_2 & 1 & y'_2x_2 & -y'_2y_2 \\ x_3 & y_3 & 1 & 0 & 0 & 0 & -x'_3x_3 & -x'_3y_3 \\ 0 & 0 & 0 & x_3 & y_3 & 1 & -y'_3x_3 & -y'_3y_3 \\ x_4 & y_4 & 1 & 0 & 0 & 0 & -x'_4x_4 & -x'_4y_4 \\ 0 & 0 & 0 & x_4 & y_4 & 1 & -y'_4x_4 & -y'_4y_4 \end{pmatrix} \begin{pmatrix} a_1 \\ a_2 \\ a_3 \\ a_4 \\ a_5 \\ a_6 \\ a_7 \\ a_8 \end{pmatrix} = \begin{pmatrix} x'_1 \\ y'_1 \\ x'_2 \\ y'_2 \\ x'_3 \\ y'_3 \\ x'_4 \\ y'_4 \end{pmatrix} \quad (2)$$

which can be solved exactly if the landmarks are not placed on a straight line. Figure 3a and b show two radiographs with four landmarks defined in each and Figure 3c the resulting subtraction. The quality of adjustment is extremely affected by the degree of precision in the positioning of the landmarks. Therefore, the registration depends on the observer placing the landmarks in both images.

Least squares problem

In our registration approach, more than four pairs of points are used. Let $N \in \mathbb{N}$ denote the number of landmarks. Then equation (1) yields an overdetermined system $(Az = b)$ of equations:

$$\begin{pmatrix} x_1 & y_1 & 1 & 0 & 0 & 0 & -x'_1x_1 & -x'_1y_1 \\ 0 & 0 & 0 & x_1 & y_1 & 1 & -y'_1x_1 & -y'_1y_1 \\ \vdots & \vdots & \vdots & \vdots & \vdots & \vdots & \vdots & \vdots \\ x_N & y_N & 1 & 0 & 0 & 0 & -x'_Nx_N & -x'_Ny_N \\ 0 & 0 & 0 & x_N & y_N & 1 & -y'_Nx_N & -y'_Ny_N \end{pmatrix} \begin{pmatrix} a_1 \\ a_2 \\ a_3 \\ a_4 \\ a_5 \\ a_6 \\ a_7 \\ a_8 \end{pmatrix} = \begin{pmatrix} x'_1 \\ y'_1 \\ \vdots \\ x'_N \\ y'_N \end{pmatrix} \quad (3)$$

In general, it is impossible to find a unique set of parameters $z = (a_1,...,a_8)^T$ that will satisfy (1) for all $n = 1, \ldots, N$. Thus, a set of such parameters $\hat{z}$ must be found which, on the average, is optimal. This optimal approximation can be determined using the least squares method[15] (see Appendix).

Figure 4 shows some registration examples based on more than four points. The data of coordinates was fitted to the model of perspective projection as described in the appendix. Although the observers placed the landmarks at totally different positions, the results of registration are nearly the same and, compared with the registration based on only four landmarks (Figure 3), the exactness of registration is improved.

Local correlation

The manual placement of corresponding points in a discrete pixel array has two disadvantages. The user is limited to the discrete positions of a digital image although structures in a subsequent radiograph may appear between these discrete coordinates. This is the major drawback. The use of a conventional computer mouse may cause additional errors. Therefore, the precision of the registration is improved by local correlation. The idea of this refinement is to cut a small template around a given landmark in the reference radiograph and use it for template matching in a small window around the corresponding landmark in the subsequent X-ray image.

Figure 5 illustrates the relationship between the window and the template. $W(m,n)$ denotes the $(M \times N)$ window extracted from the current radiograph and $T(j,k)$ the $(J \times K)$ template from the reference image. If $M \geqslant J$ and $N \geqslant K$, the local correlation is given by:[16]

$$R(m,n) = \frac{\sum_{j=1}^{J}\sum_{k=1}^{K} T(j,k) \cdot W(j-m, k-n)}{\sqrt{\sum_{j=1}^{J}\sum_{k=1}^{K} T^2(j,k)} \cdot \sqrt{\sum_{j=1}^{J}\sum_{k=1}^{K} W^2(j-m, k-n)}} \quad (4)$$

The correlation function $R(m,n)$ is computed for all $(M-J+1)\cdot(N-K+1)$ possible translations of the template T within the window W. The coordinates of the maximum value of R are used instead of the initially marked landmarks. In our approach, equation (4) is computed with sub-pixel resolution. The integers m and n are substituted by the real indices $m' = m \cdot s$ and $n' = n \cdot s$ wherein $s < 1$ denotes the stepsize. The window W is interpolated applying cubic convolution in a 4×4 neighborhood.[17]

Figure 6 visualizes the local correlation process. In this example, $M = N = 25$, $K = J = 9$ and s was set to 0.5. Six landmarks have been placed in the reference and the subsequent radiograph (a) and (b), respectively. Since the landmarks were all placed in a small region, minor misplacements by the observer course misalignments in the other image regions. This is

a **b** **c**

Figure 3 Four landmarks have been placed in the reference and the subsequent radiographs (a) and (b), respectively. The subtraction image after registration is shown in (c)

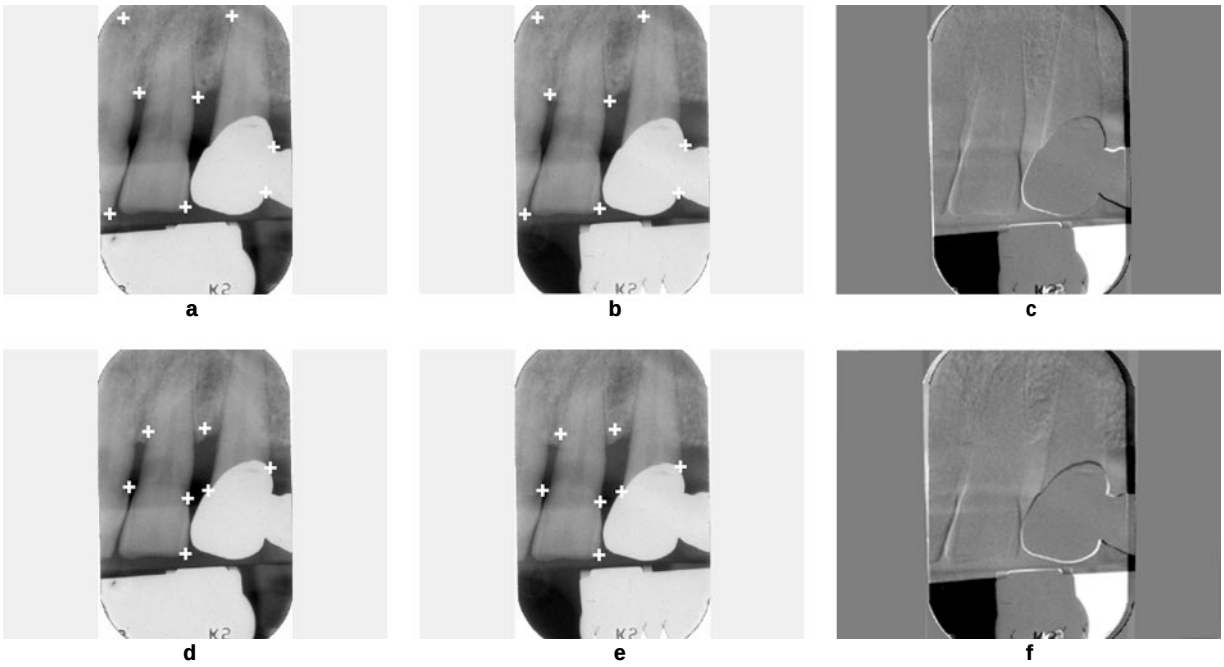

Figure 4 Other observers placed more than four landmarks into the radiographs from Figure 3. The subtraction images after registration of (a)–(b) and (d)–(e) are shown in (c) and (f), respectively. The registration based on 4 points (Figure 3c) is appreciably improved in (c) and (f)

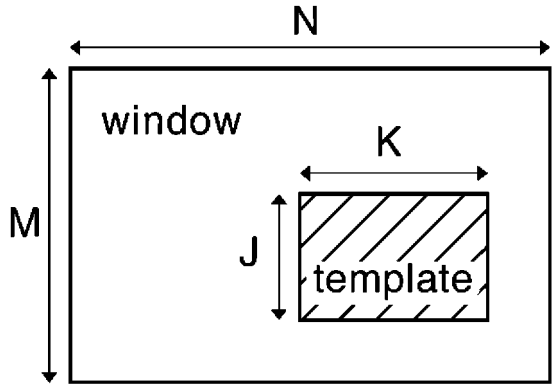

Figure 5 For local correlation, the $(J \times K)$ template is moved to all positions (m,n) within the $(M \times N)$ window and $R(m,n)$ is computed by Equation (4)

demonstrated by the subtraction (e). The window which was extracted around the upper left landmark in (b), the template corresponding to a smaller region around the upper left landmark in (a) and the result of local correlation are magnified in the three parts of (c), respectively. After local correlation, a uniform increase in intensity is visible. The coordinates of that pixel yielding the highest intensity correspond to the corrected landmark position. The local correlation is displayed for all landmarks in (d). The result of registration based on the corrected landmarks is shown in (f). The corresponding coordinates are listed in Table 2. Figure 6f demonstrates, that the correction of manually placed coordinates up to three pixels could greatly improve the quality of registration.

Leaving one out

Once the parameters a_1 to a_8 have been determined, the perspective projection described by equation (1) could be solved for each landmark (x,y) in the reference image. The distances d_n between the transformed coordinates and the manually marked corresponding points (x',y') indicate the exactness of the estimated geometric projection:

$$d = \frac{1}{N}\sum_{n=1}^{N} d_n \tag{5}$$

with:

$$d_n = \sqrt{\left(x'_n - \frac{a_1 x_n + a_2 y_n + a_3}{a_7 x_n + a_8 y_n + 1}\right)^2 + \left(y'_n - \frac{a_4 x_n + a_5 y_n + a_6}{a_7 x_n + a_8 y_n + 1}\right)^2}$$

A numerically more efficient way to determine the quality of the approximation $\hat{z}$ is given by the minimal residual:[15]

$$r = b - A\hat{z} \text{ whereas } \rho = \frac{1}{2N}||b - A\hat{z}||_2 \tag{6}$$

denotes its relative size. In other words, ρ determines the overall quality of the landmarks fitting the model of perspective projection. In our approach, this measure is used to assess the influence of single pairs of corresponding points to the final adjustment.

Because the optimization of ρ leads to an improved registration, the leaving one out method is used to enhance the adjustment precision. The leaving one out method is most widely used to determine the influence of one parameter in a set training a neural network for classification.[18] This procedure is particularly attractive when the number of samples is quite small. Here, this technique is applied to improve the quality of registration.

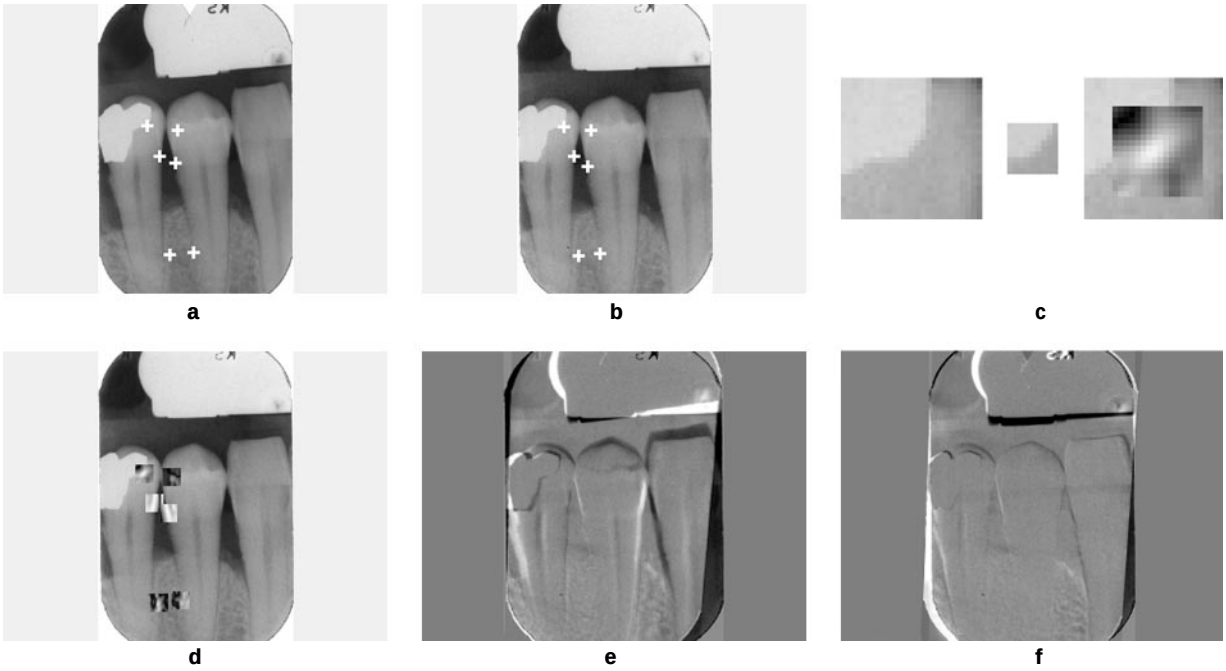

Figure 6 Six landmarks have been placed in the reference and subsequent radiographs (a) and (b) respectively. Part (c) illustrates the local correlation of the upper left landmark. A 25×25 window was extracted from the subsequent radiograph (left) and correlated with a 9×9 template taken from the reference image (middle). The correlation coefficients determined with equation (4) are mapped into this window (right). Note that the images in (c) are magnified. The results of correlation for all landmarks are superimposed in (d). The subtraction images after registration without local correlation is displayed in (e). Applying local correlation improves the quality of registration (f)

Table 2 The coordinates (x,y) and (x',y') determine the landmarks placed by observer D into the reference and subsequent image 03, respectively

Land-mark	x	y	x'	y'	m'	n'	$R(m',n')$	Δ
1	127	107	125	108	124.0	108.0	0.98081	1.00
2	138	134	134	134	133.0	136.5	0.99087	2.69
3	154	111	149	111	149.5	113.5	0.62692	2.55
4	152	140	146	143	146.0	143.0	0.99256	0.00
5	147	221	138	222	137.0	223.0	0.87550	1.41
6	168	219	157	220	158.5	222.5	0.77738	2.92

Local correlation results in the modified coordinates (m',n'). The maximum of R is calculated with equation (4). Δ determines the Euclidian distance between the pixel (x',y') and (m',n')

Suppose N points marked in both radiographs. At first, the N subsets containing $N-1$ landmarks are generated. For the initial set and all subsets the $L=N+1$ parameter vectors $\hat{z}_\ell$ and their residuals p_l with $l \in \{1,...,L\}$ are determined solving equation (8). Finding one ℓ such that $\rho_\ell \leqslant \rho_\ell$ for all $l \neq \ell$ defines the best set of parameters. This set is used as an initial set for the next leaving one out iteration. When the minimum number $N_{\min}$ of points in a set is reached or the best set equals the initial set, the iteration stops and $\hat{z}_\ell$ is used for final backprojection of the subsequent image into the geometry of the reference image.

Experimental procedure

Several authors have used artificial means to evaluate their algorithms. For instance, a digital radiograph has been digitally copied,[20] noise with a known distribution added[2] or the digital radiograph shifted and/or rotated with the aid of computer algorithms.[17] The advantage of these concepts is that the amount of transform to be corrected is known *a priori*. However, a modified digital image is still mainly related to the original. Even in an absolutely constant acquisition environment, two real radiographs differ because of several noise processes and illumination variations. If radiographs are acquired freehand, that is without individual adjustment aids, different projections of three-dimensional structures occur. In our approach, this is also considered as noise. To assess the effects caused by this kind of noise, real radiographs must be considered.

Therefore, a set of 24 pairs of *in vivo* radiographs, from the maxilla and the mandible in humans and from the mandible of dogs, was selected at random for this study. Some images contained dental implants and bridges, others teeth with and without restorations. Examples of radiographs of implants are shown in Figure 2, displaying a reference radiograph and a subsequent one taken 1 year later for the assessment of changes in the marginal bone height.

The films used were Ektaspeed Plus (Eastman Kodak Co., Rochester, NY, USA) which were placed in a film holder (Super-Bite, Hawes-Neos Dental, Gentilino, Switzerland). The holder was fitted with a silicon impression material (Optosil P, Bayer Dental, Leverkusen, Germany) which enabled it to be placed in the same position relative to the implants or teeth at the subsequent examination. There was no mechanical connection to the X-ray machine (Heliodent MD, Siemens, Bensheim,

Germany) which had a focus-film distance of approximately 30 cm. Free-hand adjustment of the tube head, aided by the directional rod of the film holder, was used to obtain a beam direction perpendicular to the longitudinal axis of implants or teeth. The films were developed automatically (AP-200, Philips Medical Systems, Stockholm, Sweden) using a total cycle time of 6 min with Röntogen developing solution (Mediquipe Scandinavia AB, Täby, Sweden) and daily monitoring.

The radiographs were digitized into 8-bit images using a CCD-camera (CCD-72E, Dage-MTI Inc., Michigan City, IN, USA) yielding 756×581 pixel elements and resolution of 560×405 TVL, a frame grabber (PixelPipeline card, Perceptics Corp., Knoxville, Tennessee, USA) and image processing software (Pixel Tools 5.0, Perceptics Corp., Knoxville, Tennessee, USA). Portrait and landscape radiographs were centered in a landscape window with 340×256 pixel. The development of image processing software was done within the Khoros environment, (Khoral Research Inc., Albuquerque, New Mexico, USA) and the statistical evaluation was performed using SAS (SAS Institute, Cary, North Carolina, USA).

Five observers (three experts KG, H-GG and WS and two non-experts, TML and a computing science student) were asked to mark corresponding points in each pair of radiographs. No further instructions were given except that at least four points, not allowed to lay on a straight line, were required for registration.

The window and template dimensions were set to 15×15 and 9×9, respectively and the stepsize s was fixed at 0.5. In addition, the leaving one out procedure was inhibited to reduce the number of landmarks below seven and not allowed to remove more than 2 points in each image.

Results

While some observers investigated the entire image, others focused their attention on assessing the marginal bone loss in specific regions. The great variation in the number and location of selected landmarks is illustrated in the left column of Figure 7. Table 3 shows the number of landmarks placed for each pair of radiographs. They vary from 4 up to 19 points with a mean of 8.975 (SD 3.055). The radiographs were registered fitting the model of perspective projection and the approximated parameters were calculated as explained above.

The parameter sets $\hat{z}_A$, $\hat{z}_B$, $\hat{z}_C$, $\hat{z}_D$ and $\hat{z}_E$ obtained from observers A, B, C, D and E, respectively are inappropriate for evaluating the observer-independence quantitatively, because equal deviations in a_i result in markedly different locations of structures in the back projected radiographs. For instance, the parameters a_7 and a_8 are much more sensitive than a_3 or a_6. Therefore, the backprojected images themselves were used to prove the observer-independence of our approach. Figure 7 shows the resulting subtractions of the transformed images based on different observers. The normalized cross-correlation coefficients were computed in a centered 150×150 window to indicate the similarity of the image data after registration.[19] The windowing was done to make sure that the only parts of the images were analysed that contained radiological information, regardless of whether the radiographs were portrait or landscape.

The intra-observer correlations are listed in Table 4. Only a few values were significantly low while most showed a high correlation between the registrations obtained by the five observers. For example, poor correlation was obtained by image 01 and observer E and image 02 and observers D and E. Comparison with Table 3 shows that in these cases only five landmarks had been placed by the observers.

Therefore, the mean and standard deviation of the correlation coefficients were computed as a function of the required number of landmarks $N_{\min}$. If one of the two observers had placed fewer landmarks in a certain image ($N < N_{\min}$), the data was not used. Table 5 summarizes the mean, standard deviation, minimum and maximum of the correlation coefficients as well as the number of correlations computed as a function of the required number of landmarks $N_{\min}$. For the first row of this table, all data was used. Considering 24 images and five observers, altogether $P = 240$ correlation coefficients were computed. Although the lowest value is about 0.144, the highest correlation is larger than 0.999 and the mean is larger than 0.9 but with a standard deviation about 0.2. On the basis that at least five landmarks are required, observer D is removed from Table 4 for image 04. This did not affect the results in general. If $N_{\min} = 6$ points, the mean of the correlation coefficients jumps to over 0.95 and the standard deviation is significantly reduced to 0.063. In this row of Table 5, the total number of correlations considered is still $P = 217$. Further increase in the number of required landmarks has only minor effects (Figure 8).

It could be summarized that our model-based registration technique is independent of the landmark positions if six or more corresponding points have been placed in both images.

Discussion

Although subtraction techniques are superior in diagnosing small changes between radiographs [2–5] automatic registration algorithms suitable for clinical radiographs are still limited to RST-movements.[9] Landmark based algorithms which are able to assess perspective projection are strongly dependent on the observer positioning the points.[10,11]

The reasons for this are twofold. On one hand, the observers usually select different image regions for placing the landmarks. Due to the summation effect in X-ray imaging, some of these regions might be less useful for the determination of perspective projection. On the other hand, the accuracy of mouse-operated positioning of the landmarks is limited.

Aagaard *et al.* have analysed the re-positioning of landmarks in identical *in vivo* radiographs from 12 patients using digitized copies.[20] The (image) landmarks

were positioned at easily recognizable image regions such as the edges of fillings, tooth apices and cementoenamel junctions and evenly distributed within each image. The precision in positioning the landmarks was described as the mean distance between the points. The divergence in placing ten

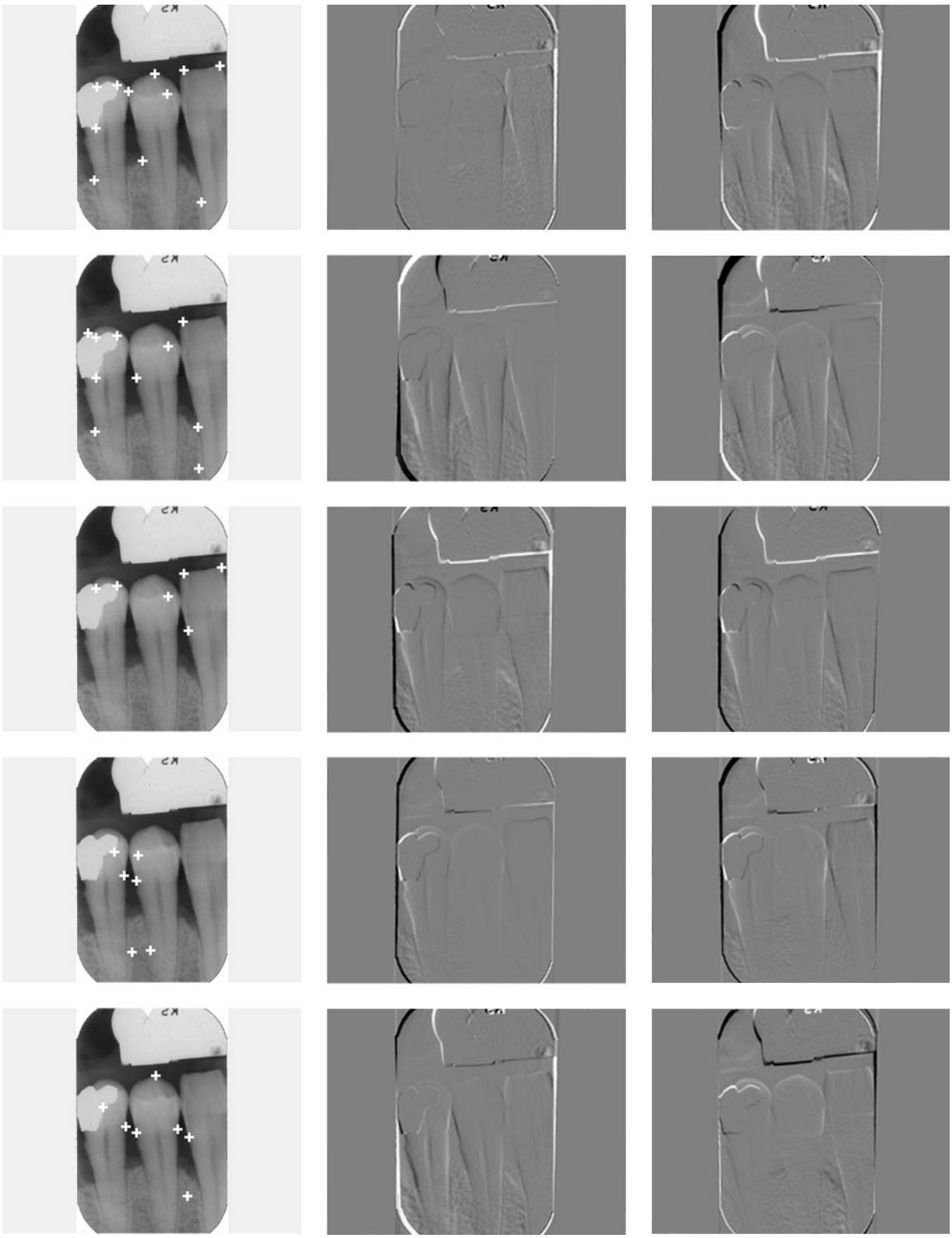

Figure 7 Observers A, B, C, D and E placed the landmarks as shown in the left column. To visualize the differences of registration, the registered subsequent images have been subtracted from each other. A−B, A−C, A−D, A−E, B−C, B−D, B−E, C−D, C−E, D−E are placed in the centre and right columns from top to bottom and from left to right, respectively

landmarks was found to be on average 1.4 pixels, considered a satisfactory result.

We have shown, that these errors may have essential effects on the geometry of the backprojected images and thus on the quality of subtraction. In the example described in Table 2, an average correction about 1.76 pixels was obtained, clearly improving the registration (Figure 6). Note that the data analysis done by Aagaard *et al*.[20] could not be transfered to the *in vivo* material used in this study. However, the misplacement occurring in different radiographs, e.g. acquired with slightly modified projection, is expected to be even larger.

In this paper, we have described a landmark-based registration technique and shown it to be observer-independent. There are three features in our approach which affect this. First the manually marked points are not mapped exactly onto each other but are used to fit a certain projection model. An analysis of intra-oral radiography showed that perspective projection approximates free-hand radiography. For this projection model at least 4 pairs of corresponding points are required. Starting with four landmarks, the precision of adjustment is improved by increasing the number of points. However, forcing the observer to place additional points when he has already marked all recognizable landmarks in the radiographs might lower

Table 3 Number of corresponding points marked in the 24 radiographs by the five observers A to E

Radiograph	*Observer*				
No.	*A*	*B*	*C*	*D*	*E*
01	13	10	6	6	5
02	12	9	6	5	5
03	11	10	6	6	7
04	13	8	6	4	7
05	12	8	6	5	8
06	12	11	6	6	7
07	9	11	6	7	6
08	9	9	6	6	9
09	11	10	7	7	8
10	12	10	7	7	9
11	16	8	7	7	7
12	12	8	6	8	9
13	19	12	7	15	13
14	17	12	7	6	8
15	10	9	6	6	8
16	14	10	6	10	9
17	8	9	6	5	7
18	14	8	6	7	7
19	10	8	6	7	7
20	14	10	6	14	12
21	14	9	6	13	10
22	13	10	7	15	9
23	13	10	7	12	8
24	17	10	6	13	10

Table 5 The cross correlation coefficients from Table 4 have been analysed

N_{min}	*P*	*Mean*	*SD*	*Min*	*Max*
4	240	0.9071	0.17852	0.1444	0.9993
5	236	0.9116	0.17662	0.1444	0.9993
6	217	0.9534	0.06265	0.6856	0.9993
7	134	0.9550	0.05989	0.6856	0.9993
8	76	0.9666	0.04971	0.7817	0.9991
9	54	0.9657	0.05133	0.8002	0.9991
10	36	0.9655	0.05360	0.8002	0.9991
11	15	0.9764	0.02387	0.9323	0.9991
12	14	0.9750	0.02418	0.9323	0.9980
13	7	0.9714	0.02770	0.9361	0.9980
14	2	0.9952	0.00401	0.9923	0.9980
15	1	0.9923	–	0.9923	0.9923

The mean, standard deviation (SD), minimum (Min) and maximum (Max) as well as the number *P* of intra-observer comparisons are determined as a function of the minimum number N_{min} of landmarks in radiograph

Table 4 The cross-correlation coefficient is computed on the subsequent images which have been transformed according to the landmarks placed by the five observers

Radiograph	*Pairs of observers*									
No.	*A–B*	*A–C*	*A–D*	*A–E*	*B–C*	*B–D*	*B–E*	*C–D*	*C–E*	*D–E*
01	0.9453	0.9822	0.9254	0.4979	0.9312	0.8663	0.4658	0.9421	0.4976	0.4647
02	0.9760	0.9920	0.1525	0.1671	0.9737	0.1443	0.1586	0.1505	0.1636	0.1625
03	0.9947	0.9791	0.9600	0.9928	0.9841	0.9649	0.9856	0.9671	0.9744	0.9566
04	0.9957	0.9879	0.6405	0.9720	0.9866	0.6351	0.9741	0.6450	0.9749	0.6478
05	0.9954	0.9837	0.9691	0.9912	0.9854	0.9758	0.9917	0.9740	0.9829	0.9842
06	0.9951	0.9976	0.9877	0.9899	0.9958	0.9951	0.9880	0.9902	0.9883	0.9827
07	0.9968	0.9960	0.8985	0.8920	0.9959	0.9045	0.8830	0.8978	0.8884	0.7667
08	0.9592	0.9601	0.8587	0.9834	0.9768	0.9014	0.9715	0.8848	0.9781	0.8672
09	0.8002	0.9826	0.7499	0.9468	0.8303	0.6856	0.7817	0.7782	0.9518	0.8444
10	0.9899	0.9895	0.8684	0.9924	0.9910	0.8640	0.9922	0.8454	0.9908	0.8749
11	0.9585	0.9944	0.9610	0.8724	0.9588	0.9099	0.8954	0.9505	0.8683	0.8865
12	0.9951	0.9518	0.9907	0.9973	0.9569	0.9916	0.9932	0.9313	0.9567	0.9887
13	0.9972	0.9987	0.9923	0.9375	0.9952	0.9891	0.9323	0.9929	0.9376	0.9551
14	0.9803	0.9802	0.9680	0.9168	0.9940	0.9874	0.9470	0.9875	0.9482	0.9580
15	0.9963	0.9959	0.7262	0.9683	0.9990	0.7153	0.9641	0.7205	0.9691	0.7542
16	0.9574	0.9885	0.9740	0.9731	0.9673	0.9658	0.9707	0.9815	0.9809	0.9982
17	0.9756	0.9753	0.3274	0.9969	0.9741	0.3419	0.9754	0.3177	0.9788	0.3275
18	0.9811	0.9973	0.9993	0.9612	0.9803	0.9819	0.9664	0.9975	0.9622	0.9643
19	0.9982	0.9980	0.9936	0.9117	0.9961	0.9935	0.9069	0.9950	0.9117	0.9016
20	0.9991	0.9887	0.9980	0.9788	0.9912	0.9977	0.9765	0.9932	0.9678	0.9792
21	0.9964	0.9943	0.9849	0.8034	0.9939	0.9887	0.8039	0.9871	0.8083	0.8028
22	0.9864	0.9974	0.9361	0.9526	0.9908	0.9590	0.9452	0.9453	0.9455	0.8959
23	0.9949	0.9989	0.9934	0.9838	0.9958	0.9975	0.9788	0.9934	0.9842	0.9832
24	0.9985	0.9963	0.9960	0.9857	0.9931	0.9985	0.9907	0.9883	0.9765	0.9949

the quality of the registration. Therefore, the number of landmarks to be set into the images is not postulated a-priori but should be higher or equal to six. Second, sloppily placed points are corrected by applying local correlation and third, wrong allocations are caught by the leaving one out optimization.

However, the landmarks used in our algorithm can not be placed indiscriminately. The local correlation must be restricted to the region of a few pixels to avoid misalignments. For example, an image landmark which was placed on the end of one screw thread or an implant might easily be connected to its neighbor by local correlation. While a few wrong landmarks can be tolerated, at least six precisely placed landmarks are required to obtain a reliable registration.

Observer-independence was proven by correlating the backprojected radiographs of different observers and not by assessing the correlation between the backprojected subsequent images and the original reference. We have explained above why we selected *in vivo* radiographs for this study. In consequence, neither the real displacement of the system components is known nor whether there are any changes in image contents. Therefore, the correlation of the back-projected subsequent image to its reference does not indicate the quality of the registration. In addition, our method it is not directly comparable with registration based on simple image correlation. A comparison based on *in vitro* material is planned for future investigation.

Although the observers placed their landmarks in totally different regions (Figure 2), the intra-observer correlation coefficients are close to 1.0 with a very low standard deviation (Table 5). Therefore, not only manually placed landmarks but also those resulting from automatic image analysis can be used for input to this registration technique. The design of suitable algorithms for automatic extraction of landmarks from dental radiographs is the aim of future research.

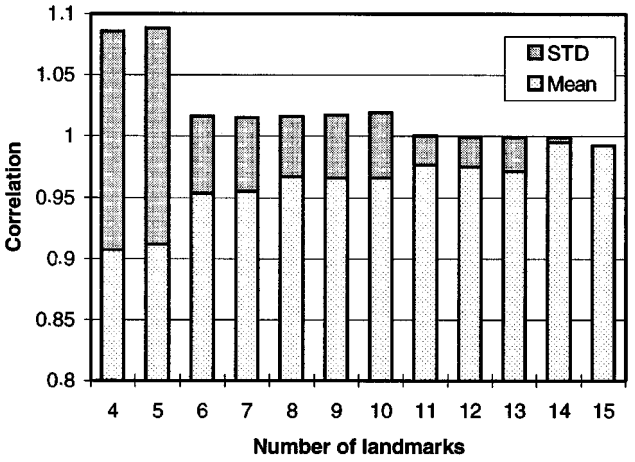

Figure 8 Increasing the number of landmarks improves the observer independence. If the observers label more than six landmarks in the images to be registered, the results of registration are highly correlated and hence they are independent of the observer placing the landmarks

It should be pointed out that the independence of the observer (or computer algorithm) placing the landmarks is strongly correlated with the precision of the registration. However, this parameter could not be determined directly with the present *in vivo* material due to changes which may occur in the structures radiographed over a time period of one year.

Acknowledgements
This work was partly supported by the German Research Community (DFG), grants: Re 427/5-1, Sp 538/1-2, Schm 1268/1-2. The additional financial support by the German Research Community (DFG), grant: Le 1108/1-1, is gratefully acknowledged. The authors would like to thank Mr Oliver Dieker for his help with the programming and Mr Thorsten Reineke for the statistical analysis.

References

1. Lehmann T, Oberschelp W, Pelikan E, Repges R. Bildverarbeitung für die Medizin: Grundlagen, Modelle, Methoden, Anwendungen. Springer-Verlag: Berlin, 1997.
2. Gröndahl HG, Gröndahl K, Okano T, Webber RL. Statistical contrast enhancement of subtraction images for radiographic caries diagnosis. *Oral Surg* 1982; **53:** 219–223.
3. Gröndahl HG, Gröndahl K. Subtraction radiography for the diagnosis of periodontal bone lesions. *Oral Surg* 1983; **55:** 208–213.
4. Brägger D, Pasquali L, Rylander H, Carnes D, Kornman KS. Computer-assisted densitometric image analysis in periodontal radiography: a methodological study. *J Clin Periodontol* 1988; **15:** 27–37.
5. Wenzel A, Warrer K, Karring T. Digital subtraction radiography in assessing bone changes in periodontal defects following guided tissue regeneration. *J Clin Periodontol* 1992; **19:** 208–213.
6. Janssen PTM, van Palenstein Helderman WH, van Aken J. The effect of in-vivo occurring errors in the reproducibility of radiographs on the use of the subtraction technique. *J Clin Periodontol* 1989; **16:** 53–58.
7. van der Stelt PF, Ruttimann UE, Webber RL. Determination of projections for subtraction radiography based on image similarity measurements. *Dentomaxillofac Radiol* 1989; **18:** 113–117.
8. Dunn SM, van der Stelt PF, Fenesy K, Shah S. A comparison of two registration techniques for digital subtraction radiography. *Dentomaxillofac Radiol* 1993; **22:** 77–80.
9. Lehmann T, Goerke C, Schmitt W, Kaupp A, Repges R. A rotation-extended cepstrum technique optimized by systematic analysis of various sets of X-ray images. *Procs SPIE* 1996; **2710:** 390–401.
10. Ruprecht D, Müller H. Image warping with scattered data interpolation methods. Technical Report 443, FB Informatik LS VII, University of Dortmund, Dortmund, 1992.
11. Bookstein FL. Morphometric tools for landmark data. Cambridge University Press, Cambridge, 1991.
12. Wenzel A. Effect of manual compared with reference point superimposition on image quality in digital subtraction radiography. *Dentomaxillofac Radiol* 1989; **18:** 145–150.

13. Reiss TH. Recognizing planar objects using invariant image features. Lecture Notes in Computer Science 676, Springer: Berlin 1993.
14. Lehmann T, Schmitt W. Determination of bone density in dental implantology by automatic subtraction of digital free-hand radiographs taken intra-orally. In: You DS, Park TW, Lee SR (eds.), Procs. 10th International Congress of Dento-Maxillo-Facial Radiology, Seoul, 1994.
15. Golub GH, van Loan CF. *Matrix Computations*. Johns Hopkins: Baltimore, 1989.
16. Pratt WK. *Digital Image Processing*. John Wiley: New York, 1978.
17. Danielson PE, Hammerin M. Note: High accuracy rotation of images. *CVGIP: Graphical Models and Image Processing* 1992; **54:** 340–344.
18. Duda RO, Hart PE. Pattern Classification and Scene Analysis. John Wiley & Sons: New York, 1973.
19. Lehmann T, Sovakar A, Schmitt W, Repges R. A Comparison of mathematical similarity measures for digital subtraction radiography. *Computers in Biology and Medicine* 1997; **27:** 151–167.
20. Aagaard E, Donslund C, Wenzel A, Sewerin I. Performance for obtaining maximal gain from a program for digital subtraction radiography. *Scand J Dent Res* 1991; **99:** 166–172.

Appendix

Using more than four landmarks to register perspective projection results in the overdetermined system of equations (3). In our approach, the least squares method is employed to find the best approximation.[15]

In equation (3) the data matrix $A \in \mathbb{R}^{2N\times 8}$ and the observation vector $b \in \mathbb{R}^{2N}$ are given. The sought vector $\hat{z}$ is of the dimension $\hat{z} \in \mathbb{R}^8$. This suggests that one strives to minimize $||A\hat{z} = b||_p$ for some suitable choice of p. For the 2-norm $p=2$ the function:

$$\phi(\hat{z}) = \frac{1}{2}||A\hat{z} - b||_2^2 \tag{7}$$

is differentiable in $\hat{z}$ and so the minimizers of ϕ satisfy the gradient equation $\nabla\phi(\hat{z}) = A^T(A\hat{z} - b) = 0$. This turns out to be an easily constructed symmetric linear system which is positive definite if A has full column rank. The gradient equation $\nabla\phi(\hat{z}) = 0$ is tantamount to solving the normal equations:

$$A^T A\hat{z} = A^T b \tag{8}$$

Since the matrix $A' = A^T A \in IR^{8\times 8}$ is symmetric positive definite, there exists a unique lower triangular matrix $C \in \mathbb{R}^{8\times 8}$ with positive diagonal entries such that $A' = CC^T$. This factorization is known as the Cholesky factorization and C is referred to as the Cholesky triangle.[15]

Using the Cholesky factorization of (8) yields:

$$A^T A\hat{z} = A'\hat{z} = (CC^T)\hat{z} = C(C^T\hat{z}) = Cz' = A^T b \tag{9}$$

and therefore, the least squares problem is reduced to the solution of the triangular systems: $Cz' = A^T b$ and $C^T\hat{z} = \hat{z}'$. Since A' determines perspective projection, the structure of A':

$$A' = A^T A = \begin{pmatrix} A'_{1.1} & 0 & A'^T_{3.1} \\ 0 & A'_{1.1} & A'^T_{3.2} \\ A'_{3.1} & A'_{3.2} & A'_{3.3} \end{pmatrix} \tag{10}$$

can be utilized for an efficient blockwise implementation of the Cholesky factorization. Note, that the blocks $A'_{i,j}$ in the diagonal with $i=j$ are squared and therefore:

$$A'_{i,j} = \sum_{k=1}^{j} C_{i.k} C^T_{j.k} \text{ with } i, j \in \{1,2,3\} \text{ and } i \geq j \tag{11}$$

Let $\sum$ abbreviate $\sum_{n=1}^{N}$, then equations (3), (10) and (11) allow an easy and numerically most efficient calculation of the least squares approximation $\hat{z} = (a_1,....,a_8)^T$ determining the eight parameters of perspective projection:

$$A'_{1.1} = \begin{pmatrix} \sum x_n^2 & \sum x_n y_n & \sum x_n \\ \sum x_n y_i & \sum y_n^2 & \sum y_n \\ \sum x_n & \sum y_n & N \end{pmatrix} = C_{1.1} C^T_{1.1}$$

$$A'_{3.1} = \begin{pmatrix} -\sum x'_n x_n^2 & -\sum x'_n x_n y_n & -\sum x'_n x_n \\ -\sum x'_n x_n y_n & -\sum x'_n y_n^2 & -\sum x'_n y_n \end{pmatrix} = C_{3.1} C^T_{3.1}$$

$$A'_{3.2} = \begin{pmatrix} -\sum y'_n x_n^2 & -\sum y'_n x_n y_n & -\sum y'_n x_n \\ -\sum y'_n x_n y_n & -\sum y'_n y_n^2 & -\sum y'_n y_n \end{pmatrix} = C_{3.1} C^T_{2.1} + C_{3.2} C^T_{2.2} = C_{3.2} C^T_{1.1}$$

$$A'_{3.3} = \begin{pmatrix} \sum (x'^2_n + y'^2_n) x_n^2 & \sum (x'^2_n + y'^2_n) x_n y_n \\ \sum (x'^2_n + y'^2_n) x_n y_n & \sum (x'^2_n + y'^2_n) y_n^2 \end{pmatrix} = C_{3.1} C^T_{3.1} + C_{3.2} C^T_{3.2} = C_{3.3} C^T_{3.3}$$